Use of FP-SPLIT Slits for Reaching High Signal-to-Noise with MAMA Detectors

Ronald L. Gilliland
April 9, 1998

ABSTRACT

A pre-flight uncertainty for STIS was the extent to which the MAMA detectors would support high signal-to-noise observations given inherently low count rates, limitations on available flat fields, and the possibility of evolution in pixel-to-pixel response stability. This ISR reports on results from STIS/SMOV-7091 Pixel-to-pixel Response Stability in which spectra were acquired at high count levels through the FP-SPLIT slits with the express purpose of demonstrating the capability of reaching signal to noise of one hundred with the MAMA detectors. A S/N ratio of about 380 per resolution element was achieved for both FUV- and NUV-MAMA data.

1. Introduction

The goal of STIS/SMOV-7091 was to demonstrate a S/N ratio of at least 100 in both FUV and NUV Echelle modes using the FP-SPLIT slits. BD+28D4211 (calibration subdwarf O star) was observed for about 8 orbits in each of E140M and E230M during mid- to late September 1997. The FP-SPLIT slits are offset from each other by a total of about 0.5” along the dispersion direction, but project to the same cross-dispersion position on the MAMAs (see Figure A.11 of the Cycle 7 STIS Instrument Handbook).

As with GHRS FP-SPLIT data, or analogous FOS data obtained by pos-targing an object in dispersion within a large aperture, the STIS FP-SPLIT data should provide many independent spectra in which offsets are obtained between the stellar spectral features and the corrupting flat-field. An assumption is that the spectra are all taken at exactly the same cross-dispersion position, which enables a solution modeling all of the data as simply the flat-field multiplied onto the stellar spectrum with unique offsets between each. If the spectra are taken at independent cross-dispersion positions, then it is not possible to solve

for a single flat-field vector and stellar vector, one would be limited to simply a *sqrt(n)* gain from averaging over the independent spectra sampling *n* different flat fields.

The observations and basic spectral extractions are discussed in § 2. § 3 provides results based on the iterative solution and a brief summary is given in § 4. An appendix provides background discussion on the limiting signal to noise expected from the iterative FP-SPLIT solutions.

2. Observations and 1-D spectral extractions.

Both the E140M and E230M spectra were obtained in each of the 5 FP-SPLIT slits (FPA, through FPE, each 0.2X0.2”), typically 7 spectra of 200-600s duration in each slit. Integrations were kept short to avoid significant Doppler smoothing within single integrations. Total integration times (summed over the five FP-SPLIT slits) were about 13,500s in each of the bands.

Since neither the FP-SPLIT slits, nor E140M had been used previously, it was considered prudent to briefly verify that target acquisitions could be done robustly into each of the 5 slits -- a special one orbit visit of 7091 executed for this purpose 18 August 1997. Target acquisitions into the FP-SPLIT slits worked well with stable count rates over the 5 slits. A substantial surprise was higher than expected global count rates by 28% for E230M and 95% for E140M. The large increase followed from better than expected sensitivity and also a substantial inter-order scattered light term that had not been included in ground-based measurements.

At global count rates of 230,000 and 102,000 per second for E140M and E230M the global count rate limit of 200,000 was exceeded; given that the stellar flux is known to be constant for this calibration star and the measurement provided an explicit determination of the rate a waiver was issued for the full observations to go forward. Since the observed object actually exceeded global screening limits, and the observations use 8 orbits per band, these data provide a very high total count level for MAMA observations.

Peak count rates were 2.2 and 2.0 per second for E140M and E230M respectively. The specified wavelengths of 1425 Å and 2707 Å provide 1150-1700 Å and 2303-3111 Å coverage at resolving powers of 35,000 and 24,000 for E140M and E230M respectively.

Although Doppler motions within individual integrations were small, it was sometimes the case that the spectrum was taken with a 1 hi-res pixel shift (and thus averaging over the hi-res flat structure) and others without such. Therefore these data are not capable of supporting an FP-SPLIT separation of flat and stellar contributions in hi-res space. All analyses to follow are based simply on using raw data re-binned to low-res pixels. No use of pre-existing flat field information has been invoked.

Just one order from each of Bands 1 and 2 (one with high count levels and an advantageous distribution of stellar features was selected) has been analyzed. Figures 1 and 2

show an echelle image for the two cases with the order analyzed marked with an arrow on the right. All analyses in this ISR use FORTRAN codes that read in .hhh/hhd format files produced with imcopy in IRAF/STSDAS from the original FITS files.

Figure 1: E230M exposure of 600s, order no. 79 covering 2562-2606 Å is analyzed.

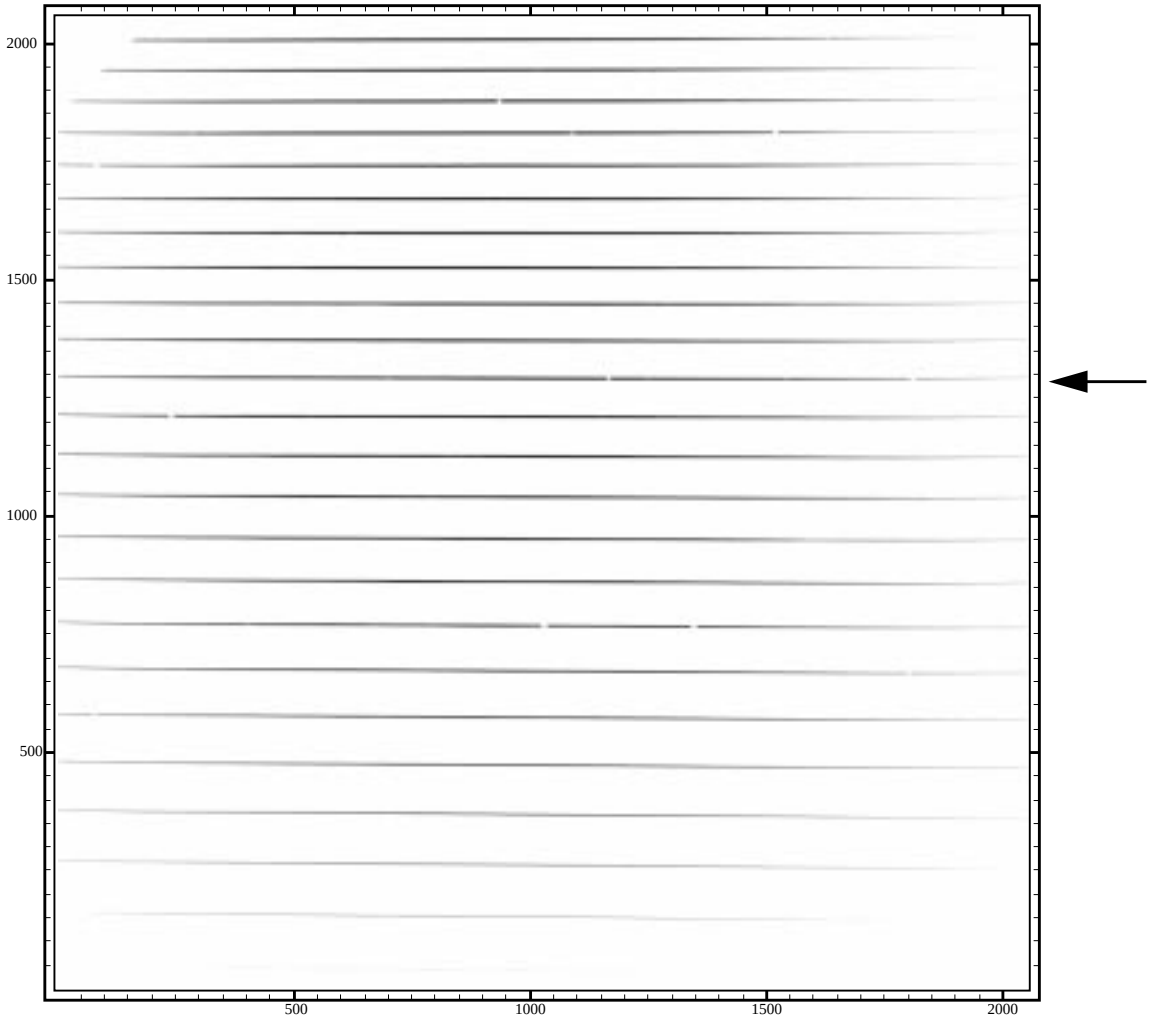

Figure 2: E140M exposure of 600s, order no. 112 covering 1313-1328 Å is analyzed.

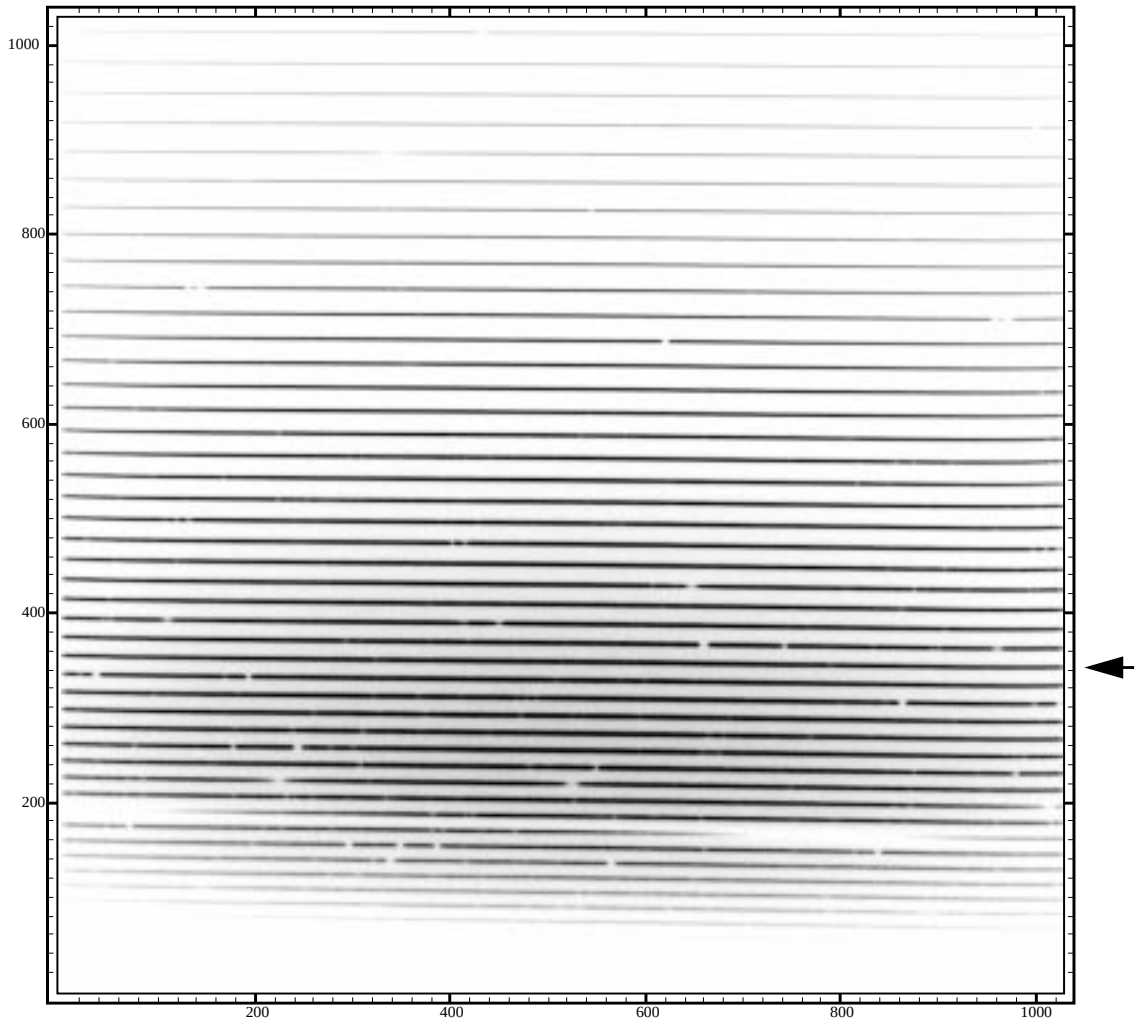

The order position in cross dispersion was found for each of the images (37 each for both bands) by fitting a gaussian to the mean over 100 columns at the center of the order. This exercise found that the spectra drifted on the detector by ~1.6 low-res pixels (E230M) and ~1.3 low-res pixels (E140M) over the eight orbits each (drift rate within a visit is up to about 0.14 low-res pixels per hour). This amount of cross-dispersion drift compromises the ability to assume a simple FP-SPLIT solution, since drifting over more than one low-res pixel will sample different pixel-to-pixel flat-field irregularities. Tables 1 and 2 provide information on slit used, rootname, exposure time and cross dispersion position for each exposure. The cross-dispersion positioning in each band shows a monotonic drift with one step about two-thirds of the way through corresponding to a visit boundary.

Table 1. E230M Spectra.

FP-SPLIT slit	Rootname[a]	T_exp (s)	y-position[b]
A	2010	376	644.027
A	2010	360	643.935
A	2icq	150	643.885
A	2idq	593	643.855
A	2040	360	643.682
A	2040	360	643.624
A	2040	360	643.587
B	2j5q	338	643.858
B	2j7q	120	643.814
B	2070	387	643.680
B	2070	360	643.658
B	2070	360	643.655
B	2070	360	643.602
B	2jkq	600	643.570
C	2090	360	643.308
C	2090	360	643.246
C	2090	360	643.226
C	2090	360	643.197
C	2k6q	110	643.191
C	2kjq	360	643.112
C	2kmq	120	643.113
C	2knq	600	643.084
D	2krq	605	642.892
D	3010	384	644.518
D	3010	360	644.346
D	3dhq	360	644.217
D	3030	360	644.132
D	3030	360	644.016
D	3040	360	643.924
E	3040	370	643.997
E	3etq	304	643.866
E	3060	150	643.805
E	3060	360	643.767
E	3060	360	643.656
E	3060	360	643.585
E	3fpq	600	643.486
E	3fqq	363	643.380

Table 2. E140M Spectra

FP-SPLIT slit	Rootname[a]	T_exp (s)	y-position[b]
A	4010	384	345.577

FP-SPLIT slit	Rootname[a]	T_exp (s)	y-position[b]
A	4010	360	345.566
A	4tbq	150	345.562
A	4tcq	600	345.546
A	4040	360	345.909
A	4040	360	345.885
A	4040	360	345.895
B	4uqq	364	345.821
B	4usq	134	345.778
B	4070	387	346.032
B	4070	360	346.050
B	4070	360	346.072
B	4070	360	346.092
B	4vlq	600	346.054
C	4090	360	346.109
C	4090	360	346.110
C	4090	360	346.093
C	4090	360	346.068
C	4whq	150	346.024
C	4wtq	360	346.370
C	4wwq	150	346.309
D	4wxq	600	346.295
D	4x2q	615	346.047
D	5010	366	345.057
D	5010	360	345.087
D	5010	411	345.088
D	5kjq	360	345.086
D	5030	360	345.379
E	5030	360	345.387
E	5040	370	345.544
E	5040	360	345.533
E	515q	134	345.474
E	5060	360	345.779
E	5060	360	345.780
E	5060	360	345.797
E	5lpq	600	345.795
E	5lqq	363	345.802

[a]First five characters of rootname: o47k0.

[b]Position of extracted order centroid in cross-dispersion.

The shape of the extracted spectra were traced by fitting a Gaussian at each pixel in cross-dispersion and stepping along the dispersion direction. Individual one-dimensional spectra were extracted as a box 7 pixels high centered on the order (with adjustments for

both shape along dispersion and image-to-image offsets). No correction was applied for scattered light -- in the sense of a simple test for S/N capability this is a correct approach.

The extracted 1-d spectra were normalized by fitting with a *sinc* function to the continuum (plus a small empirical term to account for deviations from a *sinc* function). The peak intensity of the *sinc* functions were tabulated for each spectrum. Summed over the 37 spectra for each band this provides the total peak count level, which in turn defines the Poisson limit for signal-to-noise.

Figures 3 and 4 show an extracted spectrum for each of the two bands before and after flattening with the *sinc* function fit.

Figure 3: E230M spectrum, 593s exposure. The upper panel shows the direct extraction, the lower panel shows the resulting continuum flattened spectrum.

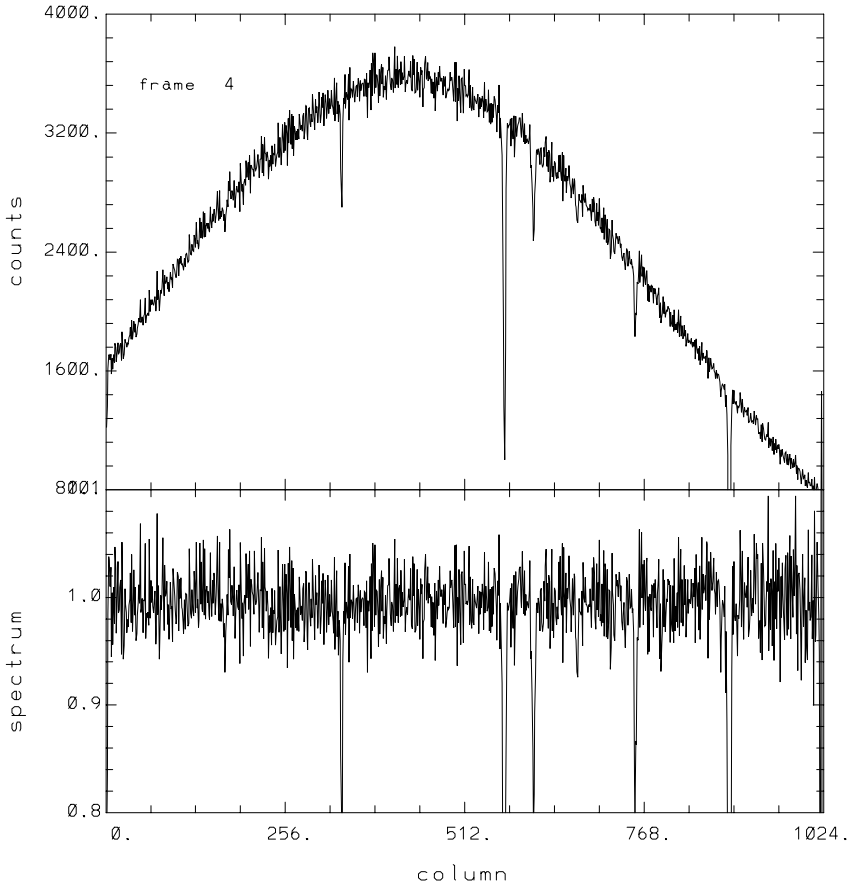

Figure 4: E140M spectrum, 600s exposure -- panels as in Fig. 3.

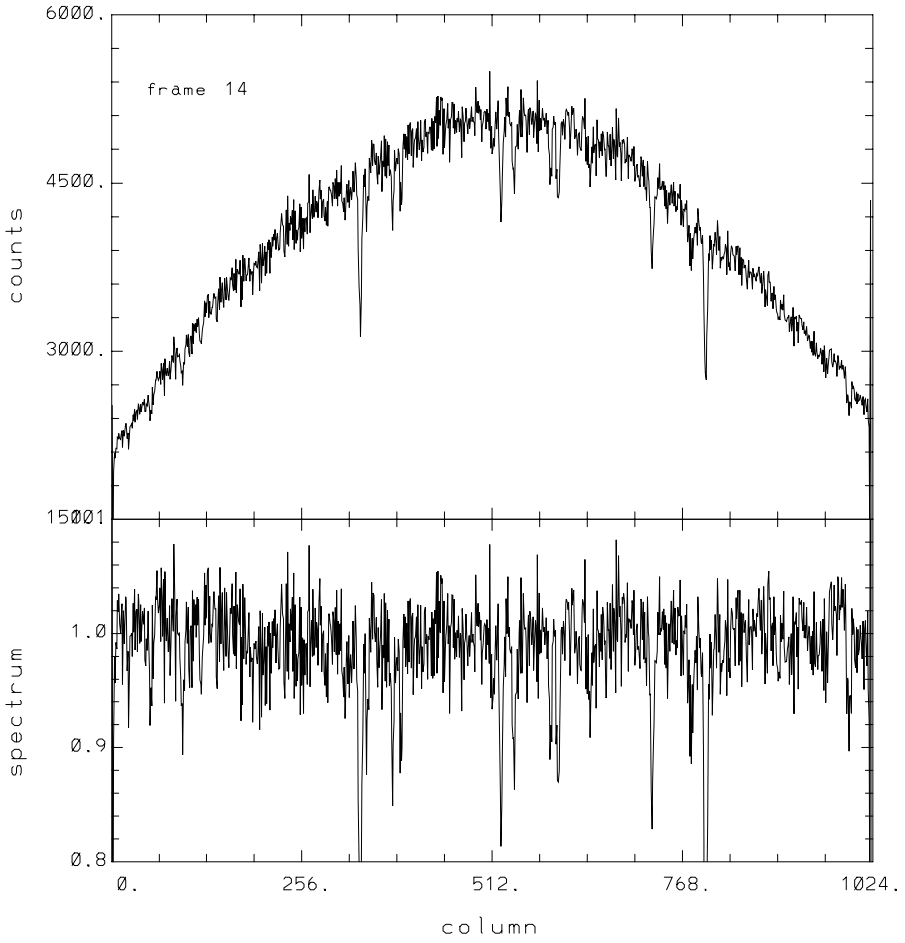

Table 3. Poisson limit S/N per wavelength pixel.

Band	Total counts/ pixel	Poisson limit S/ N
E140M	133,350	337
E230M	80,100	283

Figure 5: Average E230M spectra for two FP-SPLIT slits.

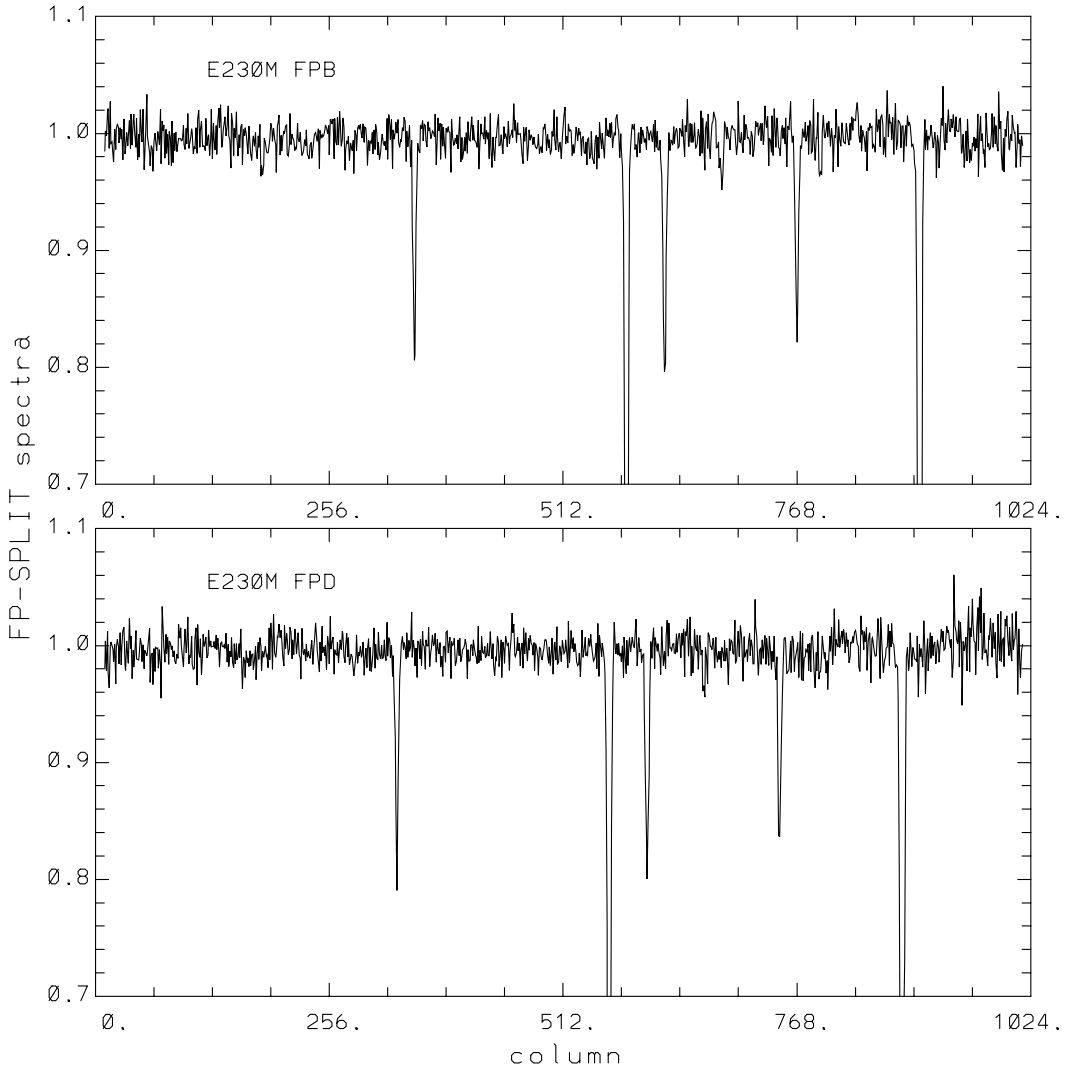

Figure 5 shows E230M spectra means for the FPB and FPD slits, the pair which gives the offset extrema. The offset between these two slits is about 19 low-res pixels, or 0.5”.

3. Analyses.

An initial guess at the stellar spectrum can be obtained simply by summing all of the individual spectra with offsets as required to line up the stellar features. Both the initial guess at the spectrum and FP-SPLIT iterative solutions require robust offset solutions which are generated using cross-correlations that include only the spectral regions showing strong, sharp lines.

S/N evaluated simply from the averaged spectra (with correct weighting based on S/N of the individual input spectra) after lining up to the nearest integer pixel are given in Table 4.

Table 4. S/N from averaged spectra.

Band	S/N
E140M	145 ± 10
E230M	175 ± 10

Figures 6 and 7 show these simply averaged E230M and E140M spectra. The range over which S/N is evaluated is indicated above the spectra.

Figure 6: Averaged E230M spectrum obtained by lining up the stellar features and applying weights proportional to signal in each component spectrum. The line at 1.0 for granularity shows the initial guess for the underlying flat field. The bar labeled S/N above the spectrum shows the line-free region used to define the signal to noise.

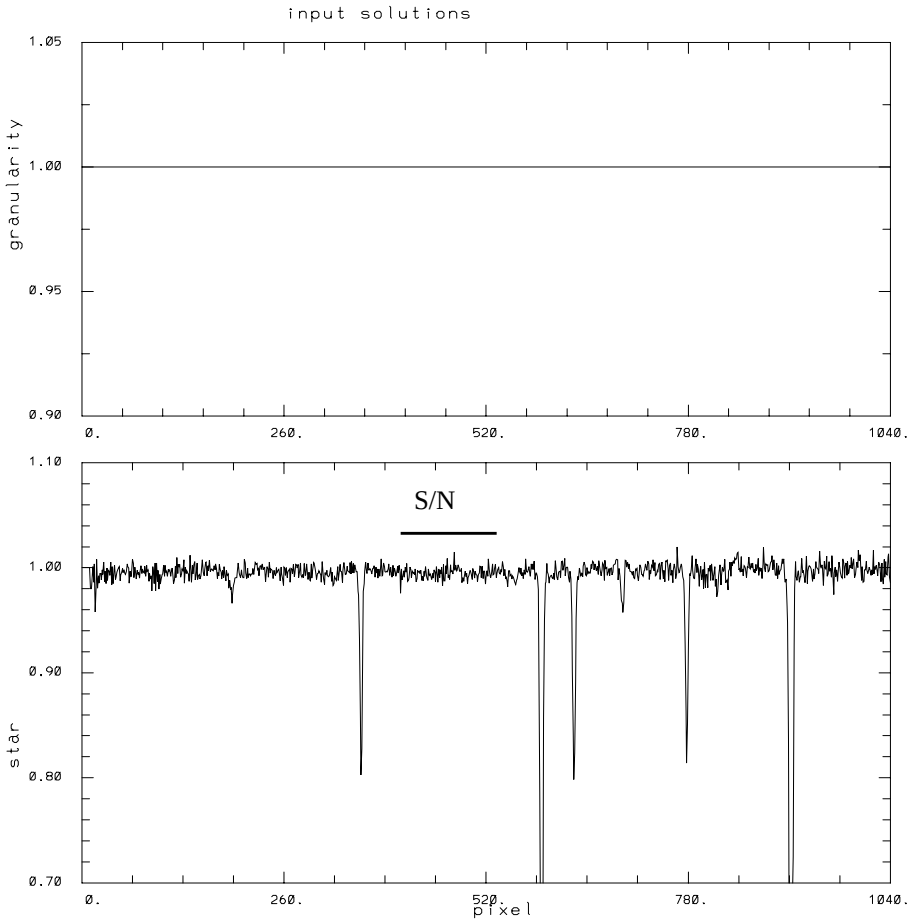

Figure 7: Averaged E140M spectrum.

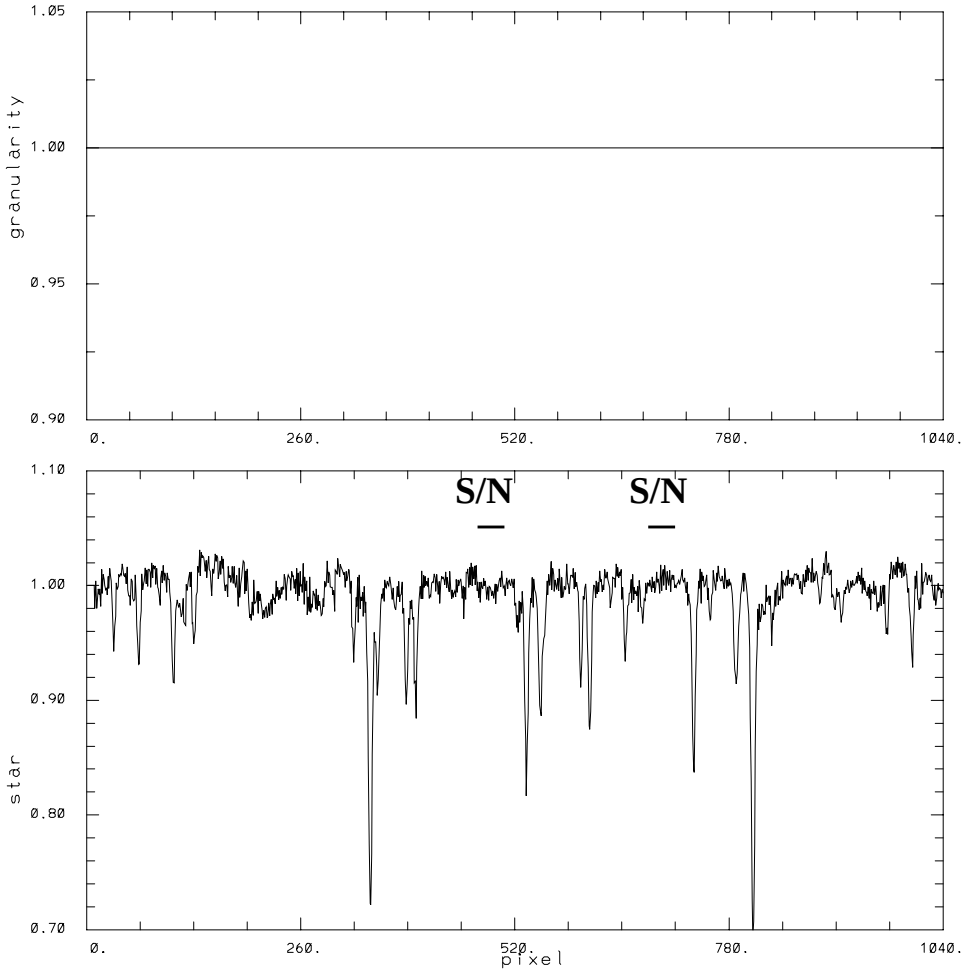

A few words are in order on how the S/N will be evaluated here. For the E230M spectrum it seems to be the case that an extensive region entirely free of stellar lines exists. In this case, assuming a good continuum flattening has been accomplished the S/N follows very simply from 1/*sqrt(rms)*, where *rms* is the standard deviation of data points around the mean of 1.0. To account for small residuals in the flattening the S/N has been evaluated two ways: (1) based on taking first differences $(d_i - d_{i+1})^2$ (which is insensitive to slow drifts), and (2) evaluating the *rms* spread about a Gaussian smoothed version of the original spectrum. (This slightly over-estimates the S/N if any small scale structure is allowed to feed through into the smoothed version. This can under-estimate the S/N, if S/N is evaluated next to a strong line which throws off the registration of smoothed and direct spectra.)

The error term on quoted S/N follows from simply the statistical stability of evaluating the S/N over only about 100 pixels. In practice the two evaluations of S/N agree with each other within the statistical uncertainty. For E140M it is more difficult to find a region that seems free of lines, but two regions summing to 100 pixels were identified. To the extent

that real lines exist the effect will be to suppress these S/N, implying that these claims should be interpreted as lower limits.

The spectra simply averaged together already comfortably exceed the goal of demonstrating S/N 100 in each band. In principle it should be possible to do much better, and nearly reach the Poisson limit by self-consistently solving for both the flat-field and stellar spectra.

An iterative solution technique originally published by Bagnuolo and Gies (1991) for the separation of (additive) binary star spectra into separate component spectra using the observation of combined spectra at a large number of orbital phases has been adopted. The technique can be easily transformed to consideration of the multiplicative case of flat-fields and stellar spectra, and was discussed for GHRS in Lambert *et al.* 1994, where we demonstrated S/N of > 900 in an exposure time of 7834s for G160M at 1465A. No fundamental changes to the approach were required in dealing with the STIS FP-SPLIT data.

The underlying assumption is that the observed data can be represented as the point-by-point product of the intrinsic stellar spectrum and corrupting flat-field:

$d_{i,l} = s_{i+osl} g_{i+ogl}$

where i = 1,1024 is pixel number along dispersion and l covers the independent offset spectra (37 in these cases). os_l and og_l are the by-spectra offsets of the stellar and granularity vectors respectively. Taking logs this is transformed to:

$dl_{i,l} = sl_{i+osl} + gl_{i+ogl}$

to match the desired additive formalism. The reader interested in the detailed equations solved and substantial related discussion should see pages 757-759 of the Lambert *et al.* 1994 paper. The goal is to arrive at the optimal separation of stellar and granularity spectra that when shifted and multiplied best represent all of the observations.

In order to initiate a solution, and in the iteration cycles it is necessary to know the offsets (in data-pixel space) of both the stellar spectra and the under-lying flat-field. In the STIS case the stellar spectra are offset in dispersion according to the distance between the 5 individual FP-SPLIT slits. The underlying flat-fields move around in pixel space as a result of the on-board Doppler correction. One proceeds by iterating equations (3) and (4) from Lambert *et al*. with periodic updates for the offsets derived by cross-correlating individual spectra with the current solution for the star (with flats divided out of individual), and flat-field (with star divided out of individual). The formalism for the GHRS allowed for a third term -- pixel response of the individual diodes, this term has not been utilized in the STIS analyses.

Weights for each of the 37 spectra are set proportional to the $(S/N)^2$ of each (could equally well just be proportional to exposure time). With 37 individual spectra the prob-

lem at hand is to solve for the 1024+19 (the 19 allows for full extent of extra spectral coverage from the FP-SPLIT offsets) pixel values of the intrinsic stellar spectrum plus the 1024+3 (the 3 allows for full extent of projected position on the detector induced by on-board Doppler compensation) pixel values of the flat-field from the 1024*37 observables. The flat-field offsets follow very closely the values predicted based on the header Doppler parameters as found using the STSDAS task calc_dop. Figures 8 and 9 show final solutions for the E230M and E140M single orders considered here. Results are shown next: (Figure 10 shows an expansion around the S/N region for E230M.)

Figure 8: Result of iterative solution for E230M. The same S/N domain shown in Figure 6 has been used throughout.

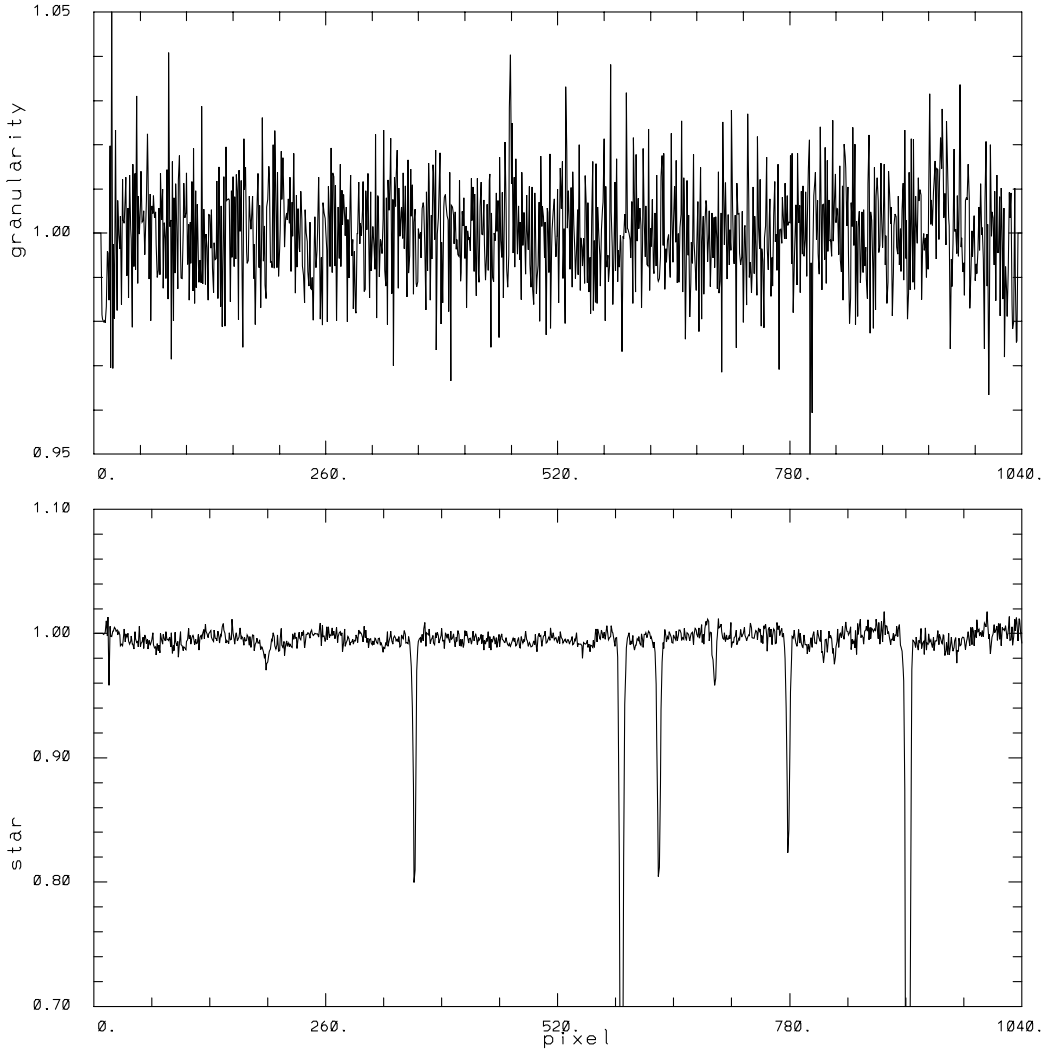

Table 5 shows the resulting S/N per wavelength pixel compared to the Poisson limit for the two bands. S/N_flat is defined in an analogous manner to S/N in the stellar spectrum, i.e. 1/*rms* and is simply meant to be indicative of the amount of derived structure.

Figure 9: Result of iterative solution for E140M. The same S/N domain shown in Fig. 7 has been used throughout.

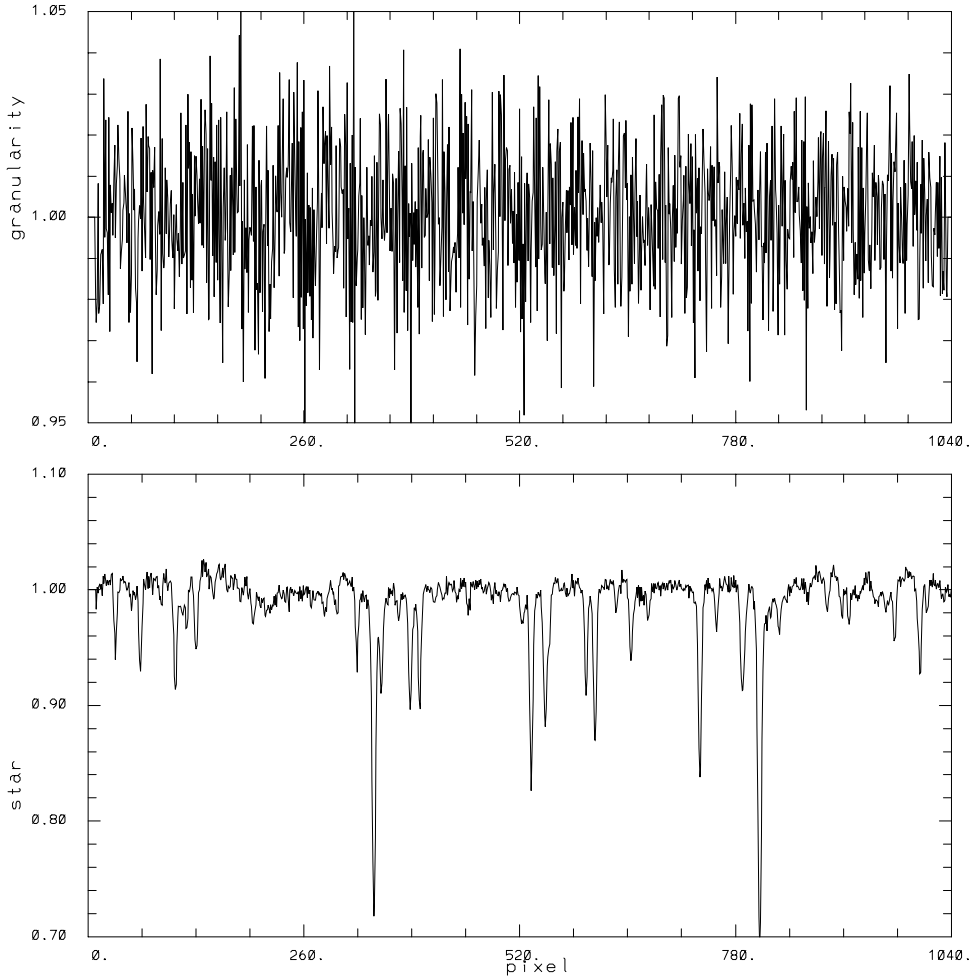

The much lower value of S/N_flat simply suggests that there is much more real structure in the flat-field solved for, than in continuum regions of the stellar spectrum.

Table 5. Solution signal to noise.

Band	Poisson limit	S/N_spec	S/N_flat
E140M	337	274 ± 20	55
E230M	283	262 ± 20	82

Figure 10: Blow-up of final stellar spectrum solution region for E230M.

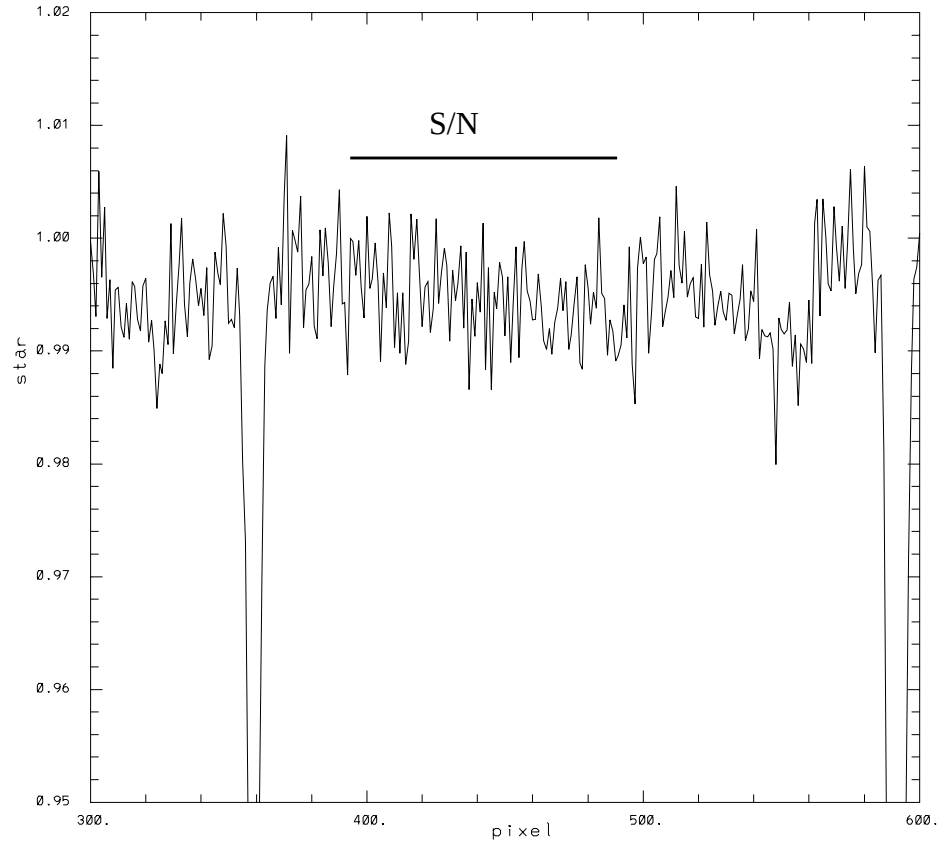

The above solutions use nearest integer (low-res) shifts of the individual spectra, and thus result in some small smearing of spectral resolution. In any experiment aimed at obtaining high S/N it is essential that resolution be verified, since smoothing in the dispersion direction whether intentional or not could contribute to artificially favorable S/N results. For the E230M case the gaussian width of the strongest spectral line in each of the individual spectra has been evaluated, and compared to the mean of that for the final solution. The strong line near pixel 900 has a mean width of 2.493 averaged over the 37 cases, and a mean line depth of -0.889. The solution vector has a gaussian width of 2.522 pixels, and a depth of -0.885. The smearing is $(2.522^2 - 2.493^2)^{1/2} = 0.38$ pixels -- about what would be expected from combining using nearest integer pixel shifts.

It is possible to use fractional pixel shifting of the spectra, at the expense of S/N loss from interpolation noise. Using Fourier domain shifting in the case of E230M a solution has been obtained with no smearing, but with S/N lowered to ~ 220 ± 20. (The fractional pixel shifting was applied only to the stellar spectra.) For E140M a stable solution has not been obtained with fractional pixel shifting. This brings up a general issue regarding these FP-SPLIT iterative solutions -- convergence is not guaranteed. Some solutions proceed smoothly while others display sensitivity to initial conditions, or details of how often during the iterations offset updates are applied.

4. Conclusions and Discussion.

Making use of the offsets provided by the FP-SPLIT slits has allowed derivation of the intrinsic stellar spectrum to S/N of ~ 270 per wavelength pixel for each band; this is essentially at the Poisson limit for E230M, and <20% below for E140M. S/N for two pixel resolution elements has been verified to go up by the expected *sqrt(2)* -- signal-to-noise of ~ 380 ± 30 per resolution element has been demonstrated for both MAMA detectors.

These data are also reported on in Kaiser *et al.* 1998, primarily from the perspective of analyzing S/N that can be obtained through direct use of available flat fields, and then averaging any independent spectra. In principle existing flat fields should be good enough to reach the S/N provided by the full iterative solution, while at the same time providing more robust results. The orders analyzed in this ISR were chosen to be ideal for processing with the iterative FP-SPLIT algorithm. Other orders, e.g. those with lines as broad, or broader than the 19 pixel FP-SPLIT separations, or that by chance have multiple lines separated by the typical distance between the FP-SPLIT spectra would pose significant challenges for the iterative solution. For example with GHRS it was possible to rotate the carousel in a nearly arbitrary manner to design optimal offset grouping, e.g. as necessary to alternatively place badly “chopped-up” and clear portions of the stellar spectrum on the same part of the detector in order to then make use of the resulting independent spectra to constrain both the stellar spectrum and corrupting flat field. The STIS FP-SPLIT slits do not provide such flexibility and a prospective user would be well advised to understand such limitations. Use of existing flat fields and then averaging together independent spectra does not face such subtleties.

A limitation (independent of FP-SPLIT considerations) to reaching high S/N with the STIS Echelles (H modes especially) while maintaining resolution follows from the rapidly changing orbital velocity vector (for objects not near the orbital pole). With the M modes to avoid intrinsic smearing at greater than 1 hi-res pixel exposures must be kept < 5-10 minutes, at H modes this would drop to < 1-2 minutes implying a substantial efficiency hit.

An additional limitation that applies in particular to use of the FP-SPLIT iterative solution follows from the awkward combination of analogue Doppler shifts in the spectral projection on the detector and discrete shifts imposed in electronics to cancel this out. Currently it is not possible to set the on-board Doppler correction off, this in turn means some spectra will always be obtained which are averaged across hi-res pixels -- these can therefore not be used to attempt an *iterative* decomposition in hi-res pixels, although a solution using existing flat fields taking into account what fraction of time was at which position during an exposure can still be developed. Given that the intrinsic resolution gain from low-res to hi-res is minor, and that the increased hi-res flat field fluctuations might be difficult to deal with in an iterative solution in any case, there are currently no plans to make Doppler compensation a selectable parameter.

5. Acknowledgments

It is a pleasure to recognize the contribution of the STIS/SMOV-7091 proposal PI, Mary Beth Kaiser, in providing a well posed observation set and general discussion. Dick Shaw provided comments and presented a AAS poster summary of this work. Steve Hulbert provided essential assistance with use of some peripheral STSDAS/STIS tasks. Stefi Baum provided valuable insights on more than one occasion and suggestions from Don Lindler were useful for reaching closure.

6. References

- Bagnuolo, W.G.,Jr. & Gies, D.R. 1991, ApJ, 376, 266-271. Tomographic Separation of Composite Spectra: AO Cassiopeiae.
- Lambert, D.L., Sheffer, Y., Gilliland, R.L., & Federman, S.R. 1994, ApJ, 420, 756-771. Interstellar Carbon Monoxide Toward ζ Ophiuchi.
- Kaiser, M.E., Bohlin, R.C., Lindler, D.J., Gilliland, R.L., & Argabright, V.S. 1998, PASP, submitted. STIS Signal-To-Noise Capabilities in the Ultraviolet.

7. Appendix.

One issue that came up with respect to these results was whether the simple Poisson limit evaluated as *sqrt*(total number of counts) should be reduced by *sqrt(2)* to account for the fact that the “available information is being split for the simultaneous determination of two quantities -- the stellar and flat-field spectra.” Numbers provided in Tables 3 and 5 assume that a *sqrt(2)* reduction **does not** apply. This point has been addressed as follows:

1. Doing a simulation with lots of intrinsic high spatial frequency structure in both the stellar and flat-field spectra and for which the added noise properties are perfectly known. The following was done:

(1) generate a stellar spectrum as 1.0+2% random gaussian deviations + a few lines superposed, (2) generate a flat as 1.0+5% random gaussian deviations, (3) take the above and create 37 independent “observed” spectra by multiplying together with the known relative offsets as in the real observations, (4) to each of the 37 spectra apply per pixel gaussian noise corresponding to 2% noise (each individual spectrum has S/N of 50, but with large structure from both star and flat on the pixel to pixel level).

Then a normal solution was performed (starting with assumption that a guess to the flat-field was known to S/N 100 -- after averaging over extraction boxes this can be exceeded in reality), and it converged to:

$S/N_{spec} = 282 \pm 12$ $S/N_{flat} = 245 \pm 12$, now derived by taking the *rms* differences versus the known inputs which have much larger and high frequency structure at the 2% and

5% level respectively. Perfect *sqrt(N)* would be S/N = 304, down by *sqrt(2)* = 215. The solution is much closer to getting back to *sqrt(N)*, than being at *sqrt(N/2)*.

2. Argument from first principles.

Assume for the moment that the real solution for the flat-field is “only” good to S/N = 200 (the *sqrt(N/2)* limit for the real E230M data).

Observe a new star in exactly the same way to a total count level of 90,000 (*sqrt(N)* implies S/N = 300 limit). Now simply use the flat-field which is good to a pixel-to-pixel value of 0.005 noise. Flat-field all of the spectra and co-register, how good is the final S/N?

Assume the following simplifying, but actually fairly close to reasonable assumptions:

(1) The combination of FP-SPLIT offsets and Doppler corrections yield spectra that are each unique in terms of relative star to flat-field positioning at the pixel level.(2) For simplicity assume 30 spectra, each with same exposure time, thus each of the 30 has a Poisson S/N level of *sqrt*(90000/30) = 54.8 or a noise level of 0.018.

The total noise level per pixel in each individual spectrum will be the quadrature sum of the flat and star limits:

noise = *sqrt*(0.018^2 + 0.005^2) = 0.0189

Since there are 30 independent spectra to average together, the final noise level is 0.0189/*sqrt*(30) = 0.0035, corresponding to a S/N of 290. This is down a bit from *sqrt(N)*, but only by 3% not *sqrt(2)*.

Now if this applies to a new observation why wouldn’t it apply to the solution to start with (any errors on the flat or the star get averaged out in the computation of the other)? If one iterates this line of thinking then the derived flat-field can be good to S/N approaching 300 in which case averaging together 30 independent measurements gets one back to a S/N of 295, i.e., very close to the simple Poisson limit of *sqrt(N)* = 300.

The *sqrt(2)* term has been shown by both direct simulation and reasonable first principles argument to not apply.